Conf-941013--41

LBL-35421
UC-414

# Lawrence Berkeley Laboratory
UNIVERSITY OF CALIFORNIA

## Accelerator & Fusion Research Division

Presented at the Applied Superconductivity Conference,
Boston, MA, October 17–21, 1994, and to be published
in the Proceedings

### A Final-Focus Magnet for PEP-II

C.E. Taylor, S. Caspi, and N. Saho

October 1994

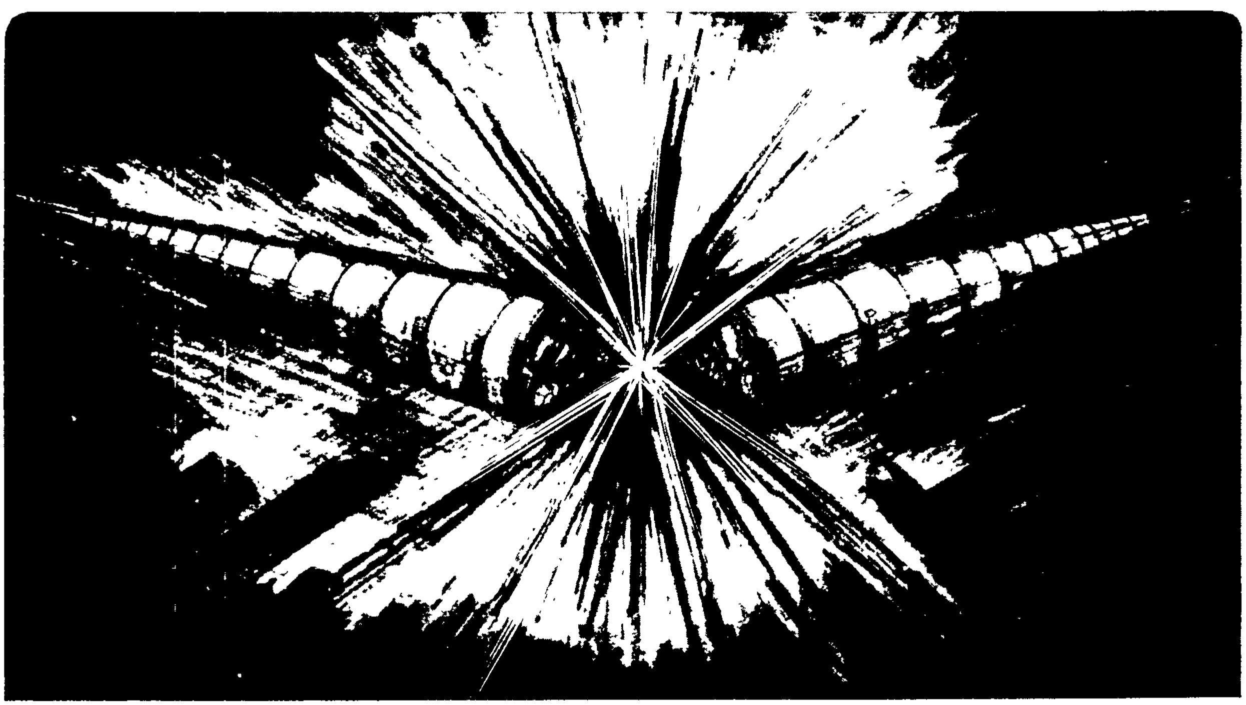

**Prepared for the U.S. Department of Energy under Contract Number DE-AC03-76SF00098**

SC-MAG-457
LBL-35421

# A Final-Focus Magnet for PEP-II*

**C. E. Taylor and S. Caspi**
Lawrence Berkeley Laboratory
University of California
Berkeley, California

**N. Saho**
Mechanical Engineering Development Laboratory
Hitachi, Ltd., Ibaraki, Japan

October 17, 1994

* This was supported by the Director, Office of Energy Research, Office of High Energy and Nuclear Physics, High Energy Physics Division U. S. Department of Energy, under Contract No. DE-AC03-76SF00098.

# A Final-Focus Magnet System For PEP-II

C. E. Taylor, S. Caspi, Lawrence Berkeley Laboratory, Berkeley, CA, USA, and
N. Saho, Mechanical Engineering Development Laboratory, Hitachi, Ltd., Ibaraki, Japan

***Abstract*--A compact quadrupole magnet has been designed for the final-focus of the 3GeV x 9GeV PEP II B-factory collider being built at SLAC. The magnet system must fit within the particle detector, has no iron, and consists of four nested separately controlled magnets: a two-layer 11.95 T/m quadrupole; a horizontal dipole; a vertical dipole; and a 1.5T solenoid. The 1.1 m long magnet must produce a highly uniform quadrupole field in the 120 mm ID beam pipe. The cryostat is 140 mm ID. (warm), 314 mm OD, and approximately 1.5 m long. The very compact cryogenic suspension system using Ti alloy plates is designed to withstand large forces due to interaction between the field of the detector solenoid and the four nested magnets. Cryogenic services and magnet leads are provided through a single flexible transfer line approximately 4m long.**

PEP-II is an asymmetric 3GeV x 9GeV electron collider ("B-factory") now under construction at SLAC. The final-focus quadrupoles must be located about 75 cm from IP within the particle detector. Both permanent and superconducting magnet options are being considered. The superconducting design presented in this paper has several advantages as compared to a permanent magnet including field adjustability; however, it is more complex. Fig. 1 is a layout of the interaction region showing the superconducting quadrupole, Q1, located inside the large 1.5T detector magnet and surrounded closely by detector elements.

Fig. 2 shows a cross-section of coils, inner bobbin, structural support tube, vacuum space, and inner and outer cryostat walls. Four nested, separately controlled magnets are assembled on a bobbin: a 2-layer 11.95T/m "cos (2Θ)" Q1 quadrupole, a 0.35T "cos (Θ)" vertical dipole (BQ1) which shifts the quadrupole magnetic center horizontally by 30 mm; a "cos (Θ)" 0.06 T horizontal dipole (BQ1-skew) for ± 5 mm of vertical adjustment of the quadrupole center; and a 1.5 T solenoid (S1) to cancel the field of the detector magnet within the beam line. An 18 mm-thick stainless steel tube fitted over the nested coils supports of the coil ends in case the 1.5T solenoid field is accidentally allowed to penetrate the coils. Table I shows parameters of the 4 windings.

TABLE I -- Coil parameters

| coil type | Q1 | BQ1 | BQ1 skew | S1 |
|---|---|---|---|---|
| gradient (T/m) | 11.95 | | | |
| Bo (T) | | .36 | .06 | 1.50 |
| magnetic length | ≈ 1 m | ≈ 1 m | ≈1 m | ≈1.1 m |
| Jop (A/sq mm) | 211 | 197 | 64 | 259 |
| Ri (mm) | 93.0 | 102.8 | 107.2 | 110.2 |
| Ro (mm) | 101.8 | 105.7 | 108.7 | 114.8 |
| coil thickness (mm) | 8.80 | 2.90 | 1.48 | 4.60 |
| E (kJ) | 14.1 | 2.9 | 0.1 | 39.1 |
| op. current (A) | 1065 | 656 | 164 | 791 |
| total turns | 355 | 190 | 131 | 1811 |
| inductance (mH) | 24.9 | 13.4 | 6.4 | 125 |

This work was supported by the Director, Office of Energy Research, Office of High Energy and Nuclear Physics, High Energy Physics Division, U.S. Department of Energy, Under Contract No. DE-AD03-76SF00098.
Manuscript received October 17, 1994

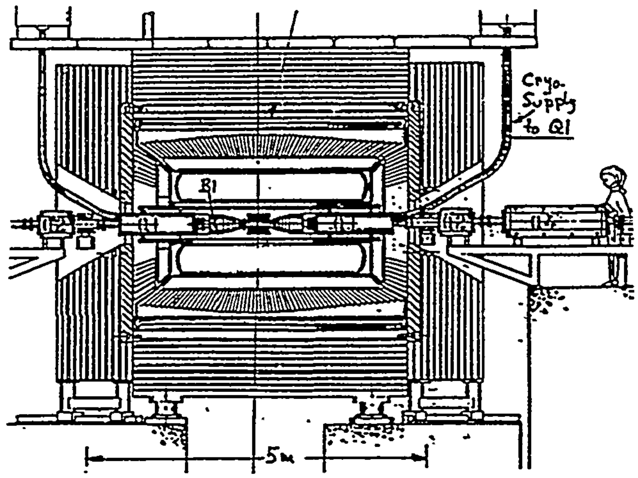

Fig. 1. Cross section view of a B factory particle detector (one of several options) showing superconducting final focus magnets

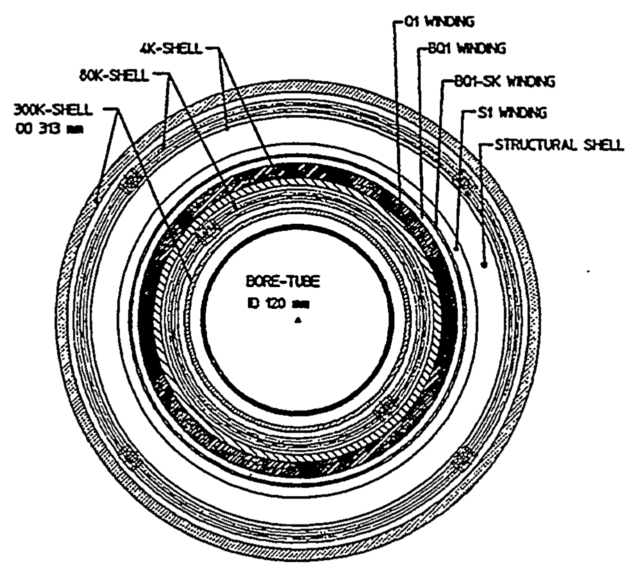

Fig. 2. Cross section of the magnet system

*Cable design* - A solder-impregnated Rutherford cable with 0.5 mm OD strands was selected for several reasons including ready availability of strand, flexibility of design, high dimensional accuracy required for Q1 and BQ1 conductor placement, and relatively small operating current. Copper strands are intermixed with the superconducting strands. to keep the copper current density (operating current/copper area) less than 500 A/sq mm. Table II shows design parameters of the several cables. Maximum field at the Q1 cable is 2.8T, which occurs if S1 is turned off while the dipoles and the detector magnet are on. Jc at 5T, 4.2K of 2400 A/sq mm is assumed for the NbTi. At an operating temperature of 4.5K, the design current margin for Q1 is then

1.5 and the temperature margin is 1.23 K; the margin for BQ1 is greater. For the four layer solenoid S1, minimum current margin is 1.4 and minimum temperature margin is 1.12K (based on the conservative assumption that the maximum field is also 2.8T; however, the maximum field in S1 will be less). The weak horizontal dipole BQ1-skew is only 1.5 mm thick and is wound with a 3-strand twisted cable. For dimensional accuracy, each coil is epoxy impregnated. Radial thickness of the cold mass including coils, intercoil spacers with helium channels, and structure is only 49 mm.

TABLE II– Cable parameters

| magnet | Q1 | BQ1 | BQ1-skew | S1 |
|---|---|---|---|---|
| cable type | rutherford | rutherford | triplet | rutherford |
| d strand(mm) | 0.5 | 0.5 | 0.5 | 0.5 |
| strand Cu/SC ratio | 1.8 | 1.8 | 1.8 | 1.8 |
| no. SC strands | 8 | 5 | 2 | 5 |
| no. Cu strands | 8 | 5 | 1 | 5 |
| total strands | 16 | 10 | 3 | 10 |
| Cu/SC area ratio | 4.60 | 4.60 | 3.20 | 4.60 |
| width (mm) | 4.00 | 2.50 | 1.08 | 2.50 |
| thickness (mm) | 1.00 | 1.00 | 1.08 | 1.00 |
| kyst angle (deg) | 0.6 | 0.5 | | |
| insul. width (mm) | 4.15 | 2.65 | 1.23 | 2.65 |
| no layers/coil | 2 | 1 | 1 | 4 |
| tot coil thk (mm) | 8.8 | 2.9 | 1.48 | 4.6 |
| coil pkg. frac | 0.71 | 0.67 | 0.29 | 0.82 |
| Jsc (A/sq mm) | 1899 | 1871 | 1171 | 2255 |
| Jcu (A/sq mm) | 413 | 407 | 366 | 490 |

*Magnetic field uniformity and winding configuration*: High field quality is required since both high energy and low energy beams must pass through the magnet with a maximum beam-beam separation of about 47 mm. For such a relatively short magnet, integral field quality is strongly determined by the placement of end turns. It is also required to keep the physical length less than 1.1m while achieving a maximum magnetic length (i.e. "short" ends). Q1 has 2-layers with 2 turn spacers in each layer and BQ1 has 4 spacers in a single layer; end turns are spaced to maximize integral field quality. Fig 3 shows a 2-dimensional cross-section of Q1 and BQ1 in the straight section and a 2-d representation of the field lines showing the shifted quadrupole center.

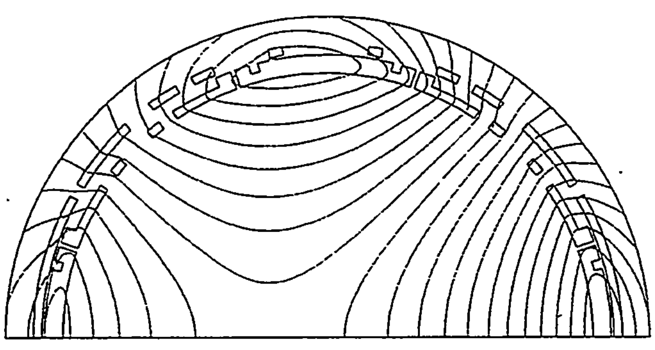

Fig. 3. Cross section through the nested 2-layer Q1 and single layer BQ1 coils with field lines showing the shifted magnetic center of the quadrupole

The integral multipole distribution, calculated assuming symmetrical ends, is shown in Fig. 4 for Q1 [2] and Fig. 5 for BQ1. (Multipole fields from the weak horizontal dipole and the solenoid are much smaller and can be neglected.)

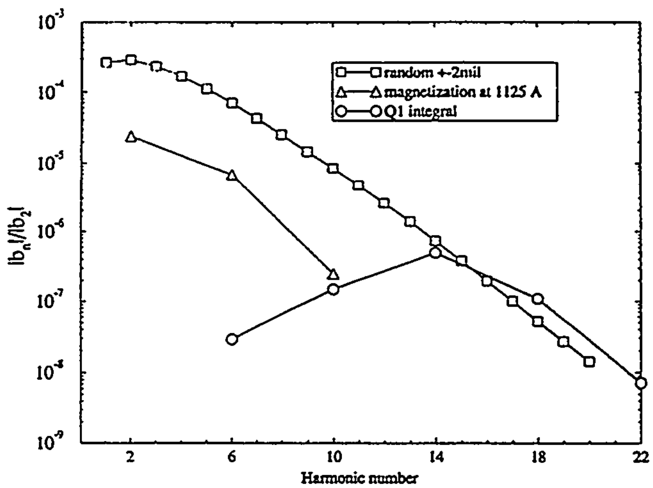


Fig. 4. Integral multipoles for quadrupole Q1

Q1 multipoles are defined as the 2n-pole field divided by the quadrupole field at r=60 mm. Integral multipoles are shown for n=6 (12-pole), n=10, 14, 18, etc. Estimated random multipoles are shown corresponding to an uncertainty in conductor placement of ± 40 μm. Also shown are estimated multipoles from superconductor magnetization for n=2, 6, 10.

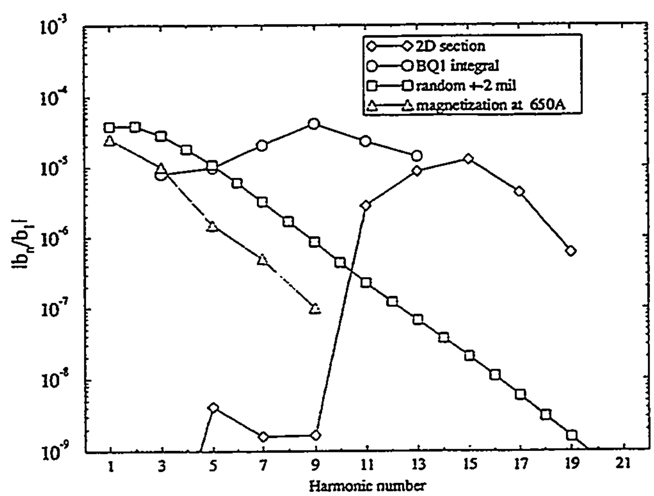


Fig. 5. Integral multipoles for vertical dipole BQ1

Similarly, Fig. 5 shows the BQ1 integral multipoles (normalized to the BQ1 dipole field at r=60 mm), estimated random multipoles, and magnetization multipoles.

The resulting field quality meets the requirements of PEP-II. Experience at LBL with six model quadrupoles for the SSC indicates that the required conductor placement accuracy is achievable with proper construction tooling.

*Forces and structural support:.* During normal operation, solenoid S1 screens the quadrupole and dipole coils from most of the field of the detector magnet; however, supports must be designed to withstand the full detector field in case S1 is accidentally turned off. In this case, large forces are developed on the end turns of the quadrupole and both dipoles in the presence of a 1.5T axial field; Fig. 6 illustrates these forces for Q1 and BQ1.

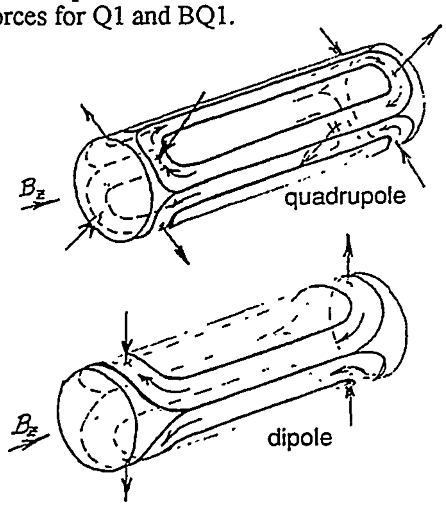


Fig. 6. Illustration of forces on end turns of Q1 and BQ1 due to immersion in a 1.5T field from the detector magnet

An 18 mm thick stainless steel tube is installed over the four magnet windings to provide support for the large bending moments developed at the ends. The radially outward forces developed by the axial magnet currents are relatively small and could be supported by a thinner tube; however, it is convenient to use a full length uniform thickness tube. In addition to forces that are internally supported by the magnet structure, the dipole sustains a large torque that must be transmitted to the cryostat outer wall through the cryogenic support struts. Also, because the screening solenoid does not extend over the entire interaction region, there is an axial force between the screening solenoid and the detector magnet that must be transmitted to the cryostat. These forces are given in Table III.

TABLE III -- forces due to 1.5 T detector field

| | F end/pole (N) | F end/pole (lb.) | direction |
|---|---|---|---|
| Q1 | 1.64E+4 | 3.68E+3 | ± radial |
| BQ1 | 1.80E+4 | 4.02E+3 | ± vertical |
| BQ1 skew | 3.01E+3 | 6.75E+2 | ± horizontal |
| S1 | 3.56E+4 | 7.97E+3 | axial |

The weight of the cold mass is 315 Kg (690 lb.) which is small compared to the magnetic forces.

*Cryostat design* : The cryostat inner radius is 70 mm and the cold mass inner radius is 88 mm leaving only 18 mm radial space which must incorporate the vacuum wall, gas-cooled radiation shield, superinsulation, and vacuum space. Similarly, the cold mass outer radius is 137 mm and cryostat outer radius is 157 mm leaving 20mm. Mechanical support is provided by a support plate located at each end of the cold mass in the vacuum space. Fig. 7 shows one of these support plates with a pattern of holes made by electrical discharge wire machining from a single 25 mm plate of material similar to a 90%Ti-6%Al-4%V alloy; these holes form effective vacuum barriers to heat conduction and thus constrict heat flow to small metal cross-sections. The remaining material forms a one piece structure having an outer ring which is firmly attached to the room temperature outer wall of the cryostat through adjustable screws; this outer ring is connected to an inner ring with four columns; two at the top and two at the bottom. The inner ring is cooled by vented helium gas to 80-100 K; four reentrant struts are connected to the inner ring at their warm end and are connected to the cold mass by two 20 mm OD pins at the cold end; the colder central member of each strut is a rectangular Ti column that is joined to the two adjacent rectangular columns; each of these two outer columns is stiffened by welding rectangular plates between them thus forming a box section around the center column. Design forces on each pin are ±18 kN (4000 lb). vertical and ±3 kN (675 lb.) horizontal. A Finite Element analysis shows that this design is satisfactory.

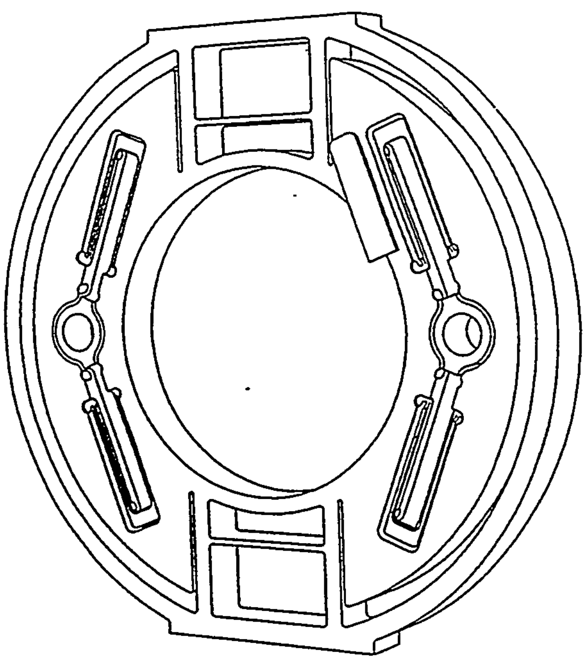

Fig. 7. Lead end support plate

Axial restraint of the cold mass with its nearly 36 kN (8000 lb) axial magnetic load is provided by two compact reentrant struts at the lead end of the cryostat.

It is necessary to assemble the two superconducting magnet systems together with the final bending magnets (permanent magnets B1) and the vertex detector in a single assembly; this complete assembly is then mounted into a 370 mm OD by ≈4 m long tube which can be inserted into its final position at the center of the detector as shown in Fig. 1. All electrical connections and cryogenic services are supplied through a flexible umbilical tube about 3-4 m long between the magnet cryostat and a services cryostat which contains magnet leads, liquid helium supply volume, instrumentation leads, and tubes for control of venting helium gas. Upon insertion of the magnet into the detector, the service cryostat, while attached to its magnet cryostat by the flexible umbilical, must be threaded through the 370 mm ID hole in the detector.

Helium from the reservour in the services cryostat is supplied to the magnet by natural circulation. In addition to helium gas that is vented through the four sets of magnet leads, helium is vented at controlled rates from each end of the magnet for cooling of the intermediate temperature ring of the Ti support plates and the inner and outer radiation shields. Liquid nitrogen is not used. During cooldown, helium is vented from the far end of the cryostat through the annular passage in the umbilical. Fig. 8 is a schematic flow diagram of the helium system showing the vent piping and control valves. Also shown are estimated flow rates and the estimated contributions of heat to the vent gas system.

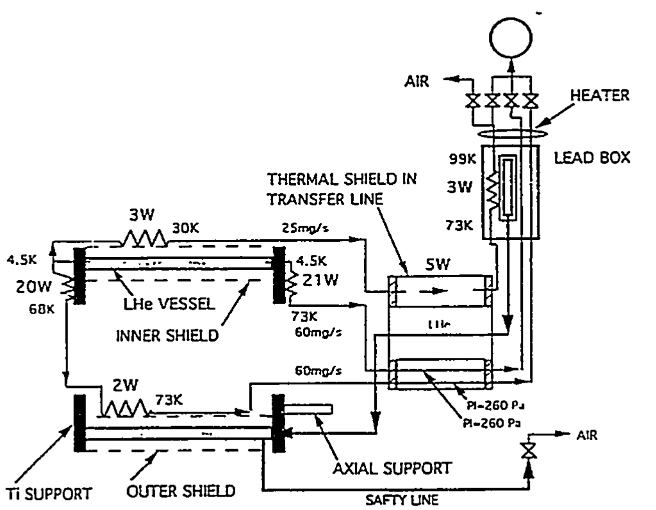


Fig. 8. Schematic of the cryostat showing helium flow circuits, estimated flow rates, and temperatures

Multilayer insulation is installed in the insulating vacuum where appropriate. Table IV shows estimated heat input in watts. Approximately 15 liters per hour of liquid helium will be required to supply the services cryostat.

TABLE IV - estimated heat input in watts.

| Item | 4.4K | 100K |
|---|---|---|
| Ti support plate - IP end | 1.2 | 20.0 |
| Ti support plate - lead end | 1.7 | 22.2 |
| Radiation shields - inner and outer | 0.2 | 6 |
| Shield support | 0 | 0 |
| Magnet cryostat subtotal | (3.2) | (48) |
| Magnet current leads (8 leads) | 6.0 | - |
| Flexible transfer line (umbilical) | 2.5 | 5.0 |
| Services cryostat | 0.6 | 3.0 |
| TOTAL | 12.1 | 56 |

Fig. 9 shows a model of the umbilical constructed from commercial stainless steel hose. The outer vacuum hose is 93 mm OD. Within this vacuum space there are two conduits containing atmospheric pressure helium: an annular passage formed by two concentric hoses, and a 13 mm minimum ID inner hose which carries the superconducting power leads as well as liquid helium supply to the magnet cryostat. Additionally, within the annular space, there are three 5.5 mm OD, 4.5 mm ID tubes that carry vent gas from radiation shields and support plates.

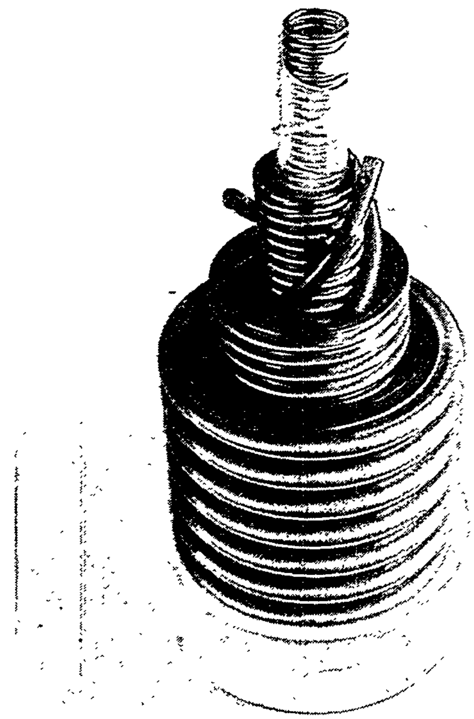

Fig. 9. Model of flexible umbilical constructed from commercial stainless steel hose.

Similar flexible lines with multiple bellows have been used before to supply services to a superconducting magnet system. [3]

*Summary* - The superconducting magnet design satisfies the severe space constraints and magnetic field uniformity requirements of the PEP II interaction region. Because of the high current density in the windings, we can include, in addition the main quadrupole Q1, a horizontal dipole BQ1, vertical dipole BQ1-skew, and a 1.5 T screening solenoid nested together in the same cryostat.

A choice has not yet been made between the permanent magnet and superconducting magnet for the project; however, it is possible that the superconducting system will be installed at a later date as an upgrade to the collider.

## REFERENCES

[1] "PEP-II An asymmetric B Factory - Conceptual Design Report", *LBL-PUB-5379 (also SLAC-418,)* June 1993

[2] Shlomo Caspi, "Q1 - A Four Wedge Superconducting Quad for the B-Factory," *SC-MAG-478,* September 29,1994

[3] Norihide Saho,"A Development of Flexible Transfer Line" - 34th Meeting on Cryogenics, November 1985 (in Japanese)